nature metabolism

LETTERS

https://doi.org/10.1038/s42255-019-0108-x

Cellular redox state constrains serine synthesis and nucleotide production to impact cell proliferation

Frances F. Diehl[1], Caroline A. Lewis[2], Brian P. Fiske[1] and Matthew G. Vander Heiden[1,3]*

The de novo serine synthesis pathway is upregulated in many cancers. However, even cancer cells with increased serine synthesis take up large amounts of serine from the environment[1], and we confirm that exogenous serine is needed for maximal proliferation of these cells. Here we show that even when enzymes in the serine synthesis pathway are genetically upregulated, the demand for oxidized NAD^+ constrains serine synthesis, rendering serine-deprived cells sensitive to conditions that decrease the cellular NAD^+/NADH ratio. Further, purine depletion is a major consequence of reduced intracellular serine availability, particularly when NAD^+ regeneration is impaired. Thus, cells rely on exogenous serine consumption to maintain purine biosynthesis. In support of this explanation, providing exogenous purine nucleobases, or increasing NAD^+ availability to facilitate de novo serine and purine synthesis, rescues maximal proliferation even in the absence of extracellular serine. Together, these data indicate that NAD^+ is an endogenous limitation for cancer cells to synthesize the serine needed for purine production to support rapid proliferation.

Many cancers exhibit altered serine metabolism[2–4], including upregulated expression of enzymes in the de novo serine-synthesis pathway[5]. The gene encoding the first enzyme in the serine-synthesis pathway, phosphoglycerate dehydrogenase (*PHGDH*), exhibits copy-number gain in some cancers[5,6], most frequently in breast cancer and melanoma[5,7]. Serine synthesis enzymes can also be transcriptionally upregulated by activating transcription factor 4 (ATF4), and many non-small-cell lung cancers exhibit ATF4-mediated PHGDH upregulation downstream of deregulated nuclear factor erythroid 2-related factor 2 (NRF2)[8]. There is also evidence that environmental serine availability can be critical for proliferation of some tumour cells[6,7,9,10]. In fact, environmental serine limitation can slow the growth of some tumours[9], and even cells with upregulated serine synthesis appear to rely on extracellular serine for optimal proliferation[10].

Serine is a precursor for many classes of biomolecules, and is a major donor of one-carbon (1C) units, which can support methylation reactions and nucleotide synthesis. One 1C unit is needed to produce deoxythymidine monophosphate (dTMP), and two 1C units are needed to produce inosine monophosphate (IMP), the precursor for both adenosine monophosphate (AMP) and guanosine monophosphate (GMP) (Supplementary Fig. 1a). Indeed, purine levels are decreased in cells cultured without exogenous serine[10], and blocking de novo serine synthesis can deplete nucleotides in some cells[11].

Why cells differentially increase serine synthesis and whether the source of intracellular serine matters for cell proliferation remains unclear. Examining the metabolic constraints of serine synthesis could provide insight. Serine consumption and synthesis differ in their demand for redox cofactors: while extracellular serine uptake does not use NAD^+, serine synthesis from glucose requires oxidation steps that consume NAD^+ and produce NADH (Supplementary Fig. 1a).

Regeneration of NAD^+ to support oxidation reactions and build biomass can be a metabolic constraint for cancer cell proliferation and tumour growth in some contexts[12–14]. This suggests that NAD^+ availability could constrain flux through the serine synthesis pathway and necessitate exogenous serine consumption. In support of this notion, withdrawing extracellular serine can increase cancer cell sensitivity to the biguanides metformin and phenformin[15], both of which inhibit NAD^+ regeneration via complex I of the mitochondrial electron transport chain (ETC)[14]. Furthermore, inhibiting NAD(H) production via the salvage pathway inhibits serine synthesis in breast cancer cells with *PHGDH* copy-number gain[16]. NAD^+ is also required to produce the 1C units needed in purine and dTMP synthesis (Supplementary Fig. 1a), raising the possibility that NAD^+ insufficiency could exacerbate the effect of serine deprivation on nucleotide synthesis. Indeed, 1C unit production is impaired in cells with defective mitochondrial respiration[17], a condition that causes decreased NAD^+ availability. The cellular NAD^+/NADH ratio can therefore dictate the metabolic processes available to cells[18], and could influence dependence on extracellular serine consumption.

We evaluated the importance of extracellular serine consumption in cells in which serine synthesis is upregulated as a result of *PHGDH* gene copy-number gain (MDA-MB-468)[5] or increased via transcriptional regulation (A549)[8]. We also examined cells with low serine synthesis (MDA-MB-231)[5,11] in which PHGDH was or was not exogenously expressed to increase serine synthesis (MDA-MB-231 pLHCX PHGDH and MDA-MB-231 pLHCX EV, respectively)[11] (Fig. 1a). In each of these cell lines, as well as in other cells with high PHGDH expression, removing serine from the medium substantially decreased proliferation (Fig. 1b and Supplementary Fig. 1b,c). PHGDH-expressing cells cultured in serine-free medium maintain robust serine synthesis, but cannot sustain the same levels of intracellular serine when extracellular serine is not available (Supplementary Fig. 1d,e). Together, these data indicate that even high expression of serine-synthesis enzymes cannot sustain maximal proliferation.

Serine deprivation has been shown to enhance the antiproliferative effects of the biguanides phenformin and metformin[15], both of which inhibit complex I of the mitochondrial ETC[14]. To examine whether increased sensitivity to serine withdrawal is generally

[1]Koch Institute for Integrative Cancer Research and Department of Biology, Massachusetts Institute of Technology, Cambridge, MA, USA. [2]Whitehead Institute for Biomedical Research, Cambridge, MA, USA. [3]Dana–Farber Cancer Institute, Boston, MA, USA. *e-mail: mvh@mit.edu

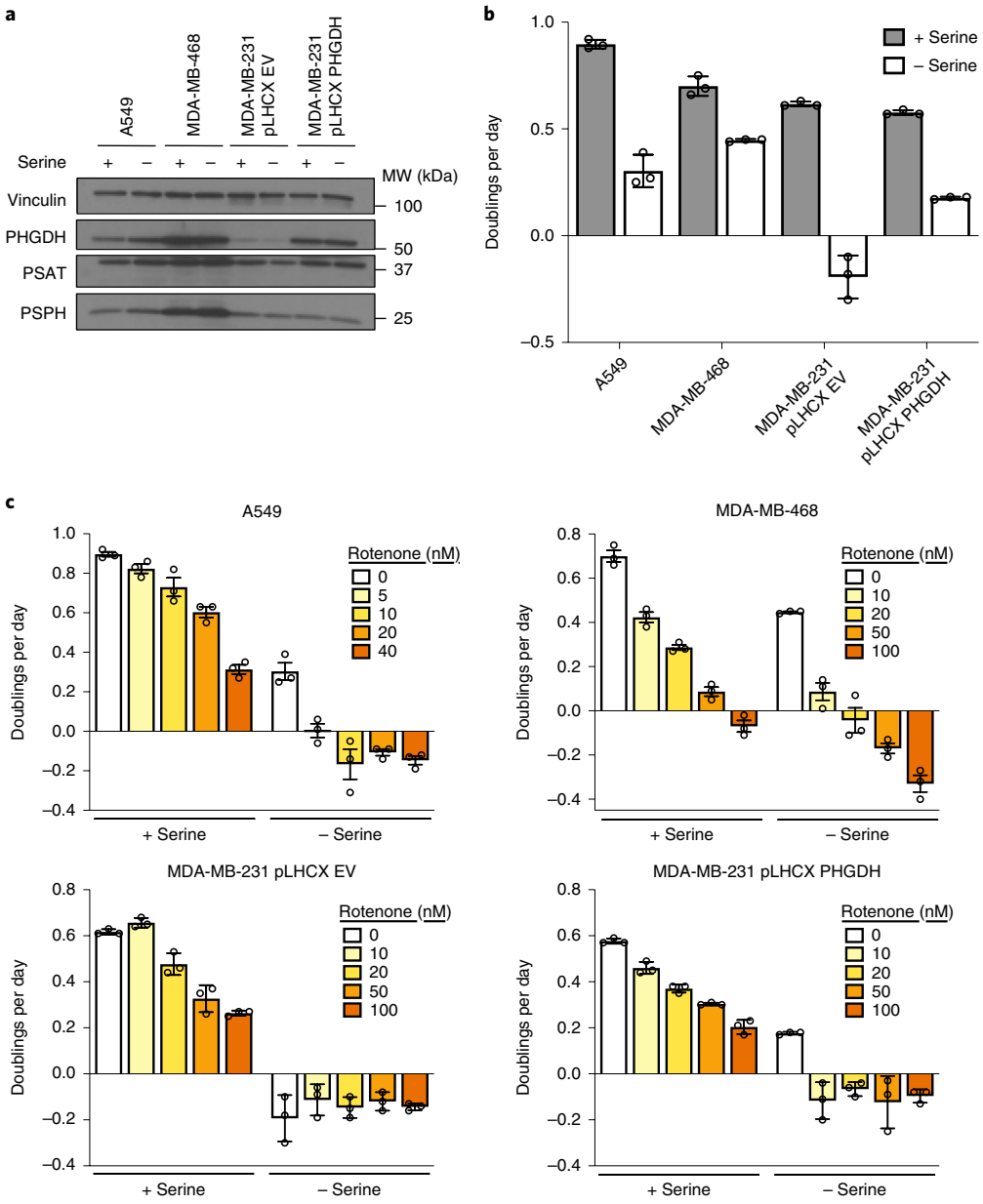

Fig. 1 | Withdrawal of exogenous serine limits proliferation and is exacerbated by inhibition of mitochondrial respiration. a, Western blot analysis of expression of serine synthesis enzymes in A549 and MDA-MB-468 cells, and in MDA-MB-231 cells with (pLHCX PHGDH) and without (pLHCX EV) PHGDH expression, as indicated. These experiments were repeated three times with similar results. MW, molecular weight. **b**, Proliferation rates of the indicated cancer cells cultured in medium with serine (+Serine), or without serine (–Serine). **c**, Proliferation rates of A549 and MDA-MB-468 cells, and of MDA-MB-231 cells with (pLHCX PHGDH) and without (pLHCX EV) PHGDH expression at the indicated concentration of rotenone, in the presence or absence of exogenous serine as indicated. Data shown are mean (± s.d.) of three biological replicates.

observed with complex I inhibitors, and whether this is affected by upregulated serine synthesis, we exposed cells to increasing concentrations of rotenone and metformin in the presence or absence of serine. Withdrawal of serine from the media increased sensitivity of cells to complex I inhibitors (Fig. 1c and Supplementary Fig. 1f). We confirmed that expression of serine-synthesis enzymes was not affected by mitochondrial inhibition (Supplementary Fig. 2a). These data suggest that extracellular serine can be limiting for cell proliferation, even in cells with increased serine synthesis, and that this limitation can be exacerbated by inhibiting mitochondrial complex I.

Production of nucleotides is an important fate of serine carbon that supports proliferation[10,11,19]. To assess whether cells prefer to use either extracellular serine or newly synthesized serine to produce nucleotides, we traced the fate of [6-^{13}C]glucose or [3-^{13}C]serine. For cells cultured in [6-^{13}C]glucose, newly synthesized serine has a mass value of $M+1$, and generates an $M+1$ 1C unit. [6-^{13}C]glucose can also label the ribose backbone of nucleotides. For cells cultured in [3-^{13}C]serine, consumed serine has a mass of $M+1$, and generates an $M+1$ 1C unit (Supplementary Fig. 1g). 1C units contribute to pyrimidine synthesis only when used to add a methyl group to make dTMP. Thus, when cells are cultured in the presence of [6-^{13}C]glucose, comparing $M+1$ labelling of dTMP and dCMP reveals whether 1C units are derived from serine that was synthesized from glucose. dTMP labelling from [3-^{13}C]serine in turn reflects dTMP production from exogenous serine. Consistent with only a small fraction of the serine in MDA-MB-468 cells being derived

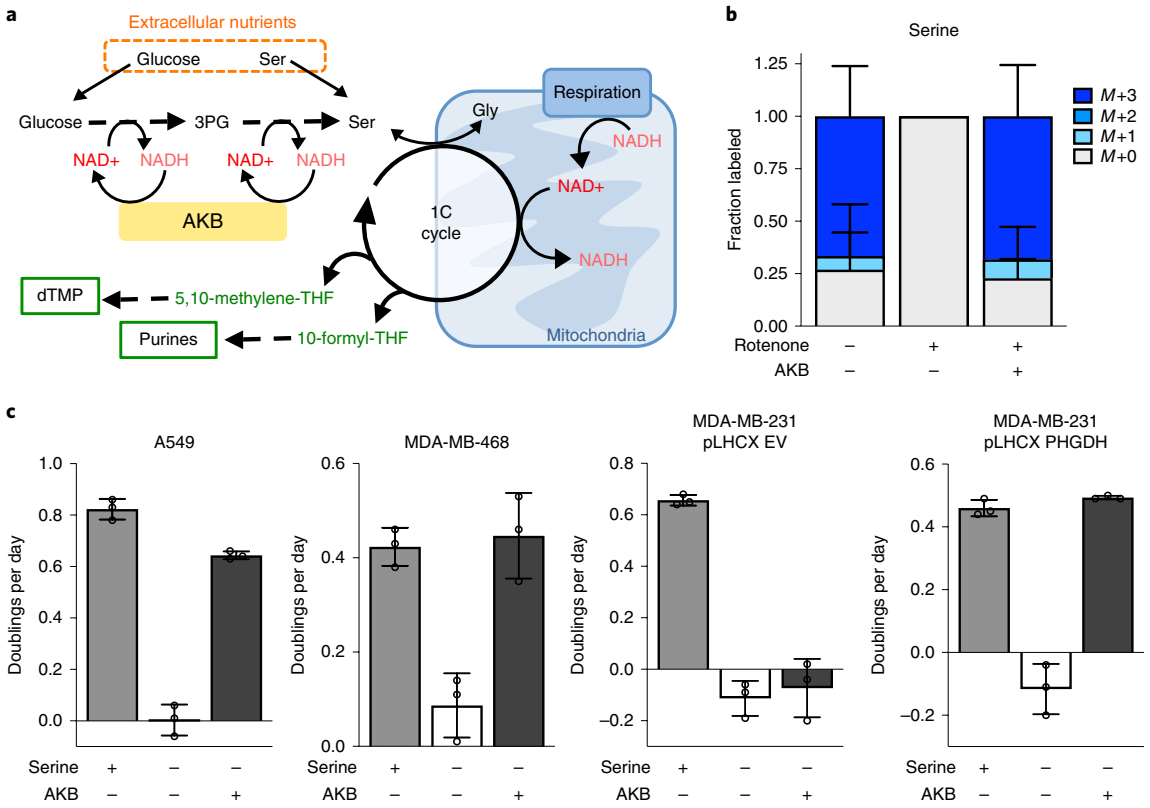

Fig. 2 | Electron acceptor availability limits serine synthesis and cell proliferation. a, Schematic showing the relationships among serine synthesis, the 1C cycle and nucleotide synthesis (dTMP and purines), highlighting the NAD^+-consuming steps involved in serine synthesis and 1C unit generation. Also shown is how NAD^+ can be regenerated from NADH via mitochondrial respiration, or by the reduction of α-ketobutyrate (AKB) to α-hydroxybutyrate. 3PG, 3-phosphoglycerate; THF, tetrahydrofolate. **b**, Fractional labelling of serine from [U-^{13}C]glucose in A549 cells cultured for 48 h in serine-free medium with or without 20 nM rotenone, and with or without AKB as indicated. Labelling was determined by liquid chromatography–mass spectrometry (LCMS) analysis. **c**, Proliferation rates of the specified cells cultured in medium containing 20 nM rotenone, with or without serine and AKB, as indicated. Data shown are mean (± s.d.) of three biological replicates.

from glucose when extracellular serine is available (Supplementary Fig. 1e), the increased amount of dTMP labelled from [6-^{13}C]glucose compared to dCMP labelled from [6-^{13}C]glucose (resulting from [6-^{13}C]glucose-derived 1C units) is small relative to the amount of dTMP labelled from extracellular serine (Supplementary Fig. 1g). This argues that cells do not preferentially use serine derived from one source for 1C unit production. It also raises the question of why extracellular serine is important for proliferation, even when cells have genetically upregulated synthesis and unlimited access to glucose. Because glucose is abundant in cell-culture medium and these cells excrete most glucose carbon as lactate[1], serine synthesis is unlikely to be limited by carbon substrate availability.

De novo serine synthesis and serine uptake have different redox cofactor requirements. Unlike the consumption of exogenous serine, serine production from glucose involves two oxidation reactions that consume NAD^+ and produce NADH, and thus requires transfer of electrons to a waste product for every serine molecule produced (Fig. 2a). Flux through serine synthesis should therefore be sensitive to the cellular NAD^+/NADH ratio. Of note, mitochondrial respiration allows transfer of electrons to oxygen and regenerates NAD^+ from NADH. Thus, a decreased NAD^+/NADH ratio could explain why cells without access to exogenous serine are more sensitive to complex I inhibition. To test this possibility, we compared serine production from [U-^{13}C]glucose in cells with and without complex I inhibition (Supplementary Fig. 1d). While untreated serine-deprived cells displayed robust serine labelling from glucose, rotenone treatment completely eliminated [U-^{13}C]glucose incorporation into serine (Fig. 2b). As expected, rotenone treatment decreased the cellular NAD^+/NADH ratio (Supplementary Fig. 4a). We next supplemented rotenone-treated cells with the exogenous electron acceptor α-ketobutyrate (AKB), which can be reduced to α-hydroxybutyrate (AHB) to regenerate NAD^+ (Supplementary Fig. 2b)[13]. Indeed, providing AKB restored serine synthesis from glucose in rotenone-treated cells (Fig. 2b). We confirmed that cells took up AKB and used it to produce AHB (Supplementary Fig. 2c), and that AKB supplementation restored the NAD^+/NADH ratio (Supplementary Fig. 4a), but did not cause cells to further upregulate expression of serine synthesis enzymes (Supplementary Fig. 2a). Addition of AKB also rescued proliferation of rotenone-treated and metformin-treated cells cultured in the absence of exogenous serine (Fig. 2c, Supplementary Fig. 2d,e and Supplementary Fig. 5b). Together, these data indicate that NAD^+ availability can limit serine synthesis and cell proliferation, particularly when the ability to transfer electrons to oxygen is impaired.

Producing 1C units for nucleotide synthesis relies on functional mitochondrial respiration because mitochondrial NAD^+ is needed to generate 1C units[17] (Fig. 2a), as is the case in most cells[20]. Since serine is a major 1C unit donor, impaired serine synthesis following complex I inhibition could exacerbate a decrease in 1C unit production. To test this possibility, we assessed how metabolite levels change in cells cultured in serine-replete compared with serine-free medium, with or without rotenone treatment. Indeed, purine nucleotides were among the most-depleted metabolites in serine-deprived cells, and rotenone treatment further exacerbated

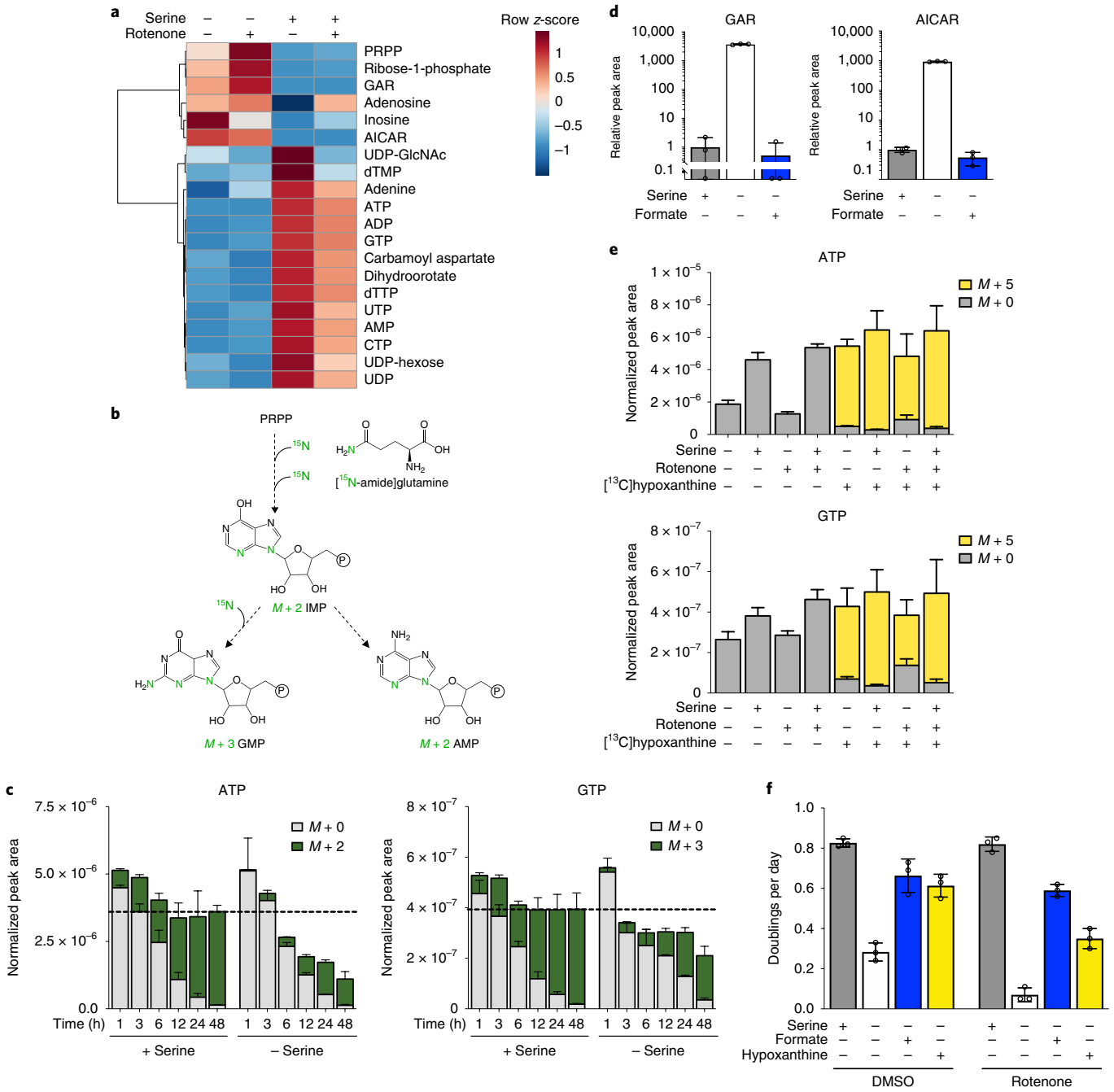

Fig. 3 | Purine nucleotide production downstream of serine metabolism constrains cell proliferation when NAD$^+$ regeneration is impaired. a, Hierarchical clustering and heat map indicating relative metabolite levels measured using LC–MS from A549 cells cultured for 48 h in medium with or without serine and with or without 20 nM rotenone, as indicated. **b**, Schematic showing how the ^{15}N label is incorporated from [amide-^{15}N]glutamine into the purines AMP and GMP. Two ^{15}N labels are incorporated into newly synthesized AMP, while three ^{15}N labels are incorporated into newly synthesized GMP. PRPP, phosphoribosyl pyrophosphate. **c**, Total levels and labelling of ATP and GTP from [amide-^{15}N]glutamine, as determined by LC–MS in A549 cells cultured in medium with serine, or in medium lacking serine for the indicated times. **d**, Levels of the purine synthesis intermediates GAR and AICAR measured using LC–MS in A549 cells cultured with or without serine and with or without formate as indicated. GAR and AICAR each precede steps in purine synthesis that involve addition of a 1C unit derived from formate. **e**, Total levels and labelling of ATP and GTP from [5-^{13}C]hypoxanthine in A549 cells cultured with or without serine, 20 nM rotenone, and [5-^{13}C]hypoxanthine, as indicated. Metabolites were analysed by LC–MS. **f**, Proliferation rates of A549 cells cultured with or without serine, formate and/or hypoxanthine, and treated with DMSO or 20 nM rotenone as indicated. Data shown are mean (± s.d.) of three biological replicates.

purine nucleotide depletion (Fig. 3a). To directly test whether de novo purine synthesis is impaired in serine-deprived cells, we measured the incorporation of ^{15}N from [amide-^{15}N]glutamine into purines. Because the amide nitrogen of glutamine is incorporated in two steps of AMP synthesis and three steps of GMP synthesis, any newly synthesized adenylate or guanylate nucleotides have mass values of $M+2$ and $M+3$, respectively (Fig. 3b). Cells cultured in serine-replete medium used de novo synthesis to turn over their purine pools by 48 h (Fig. 3c and Supplementary Fig. 3a). In contrast, cells cultured in serine-free medium had decreased de novo

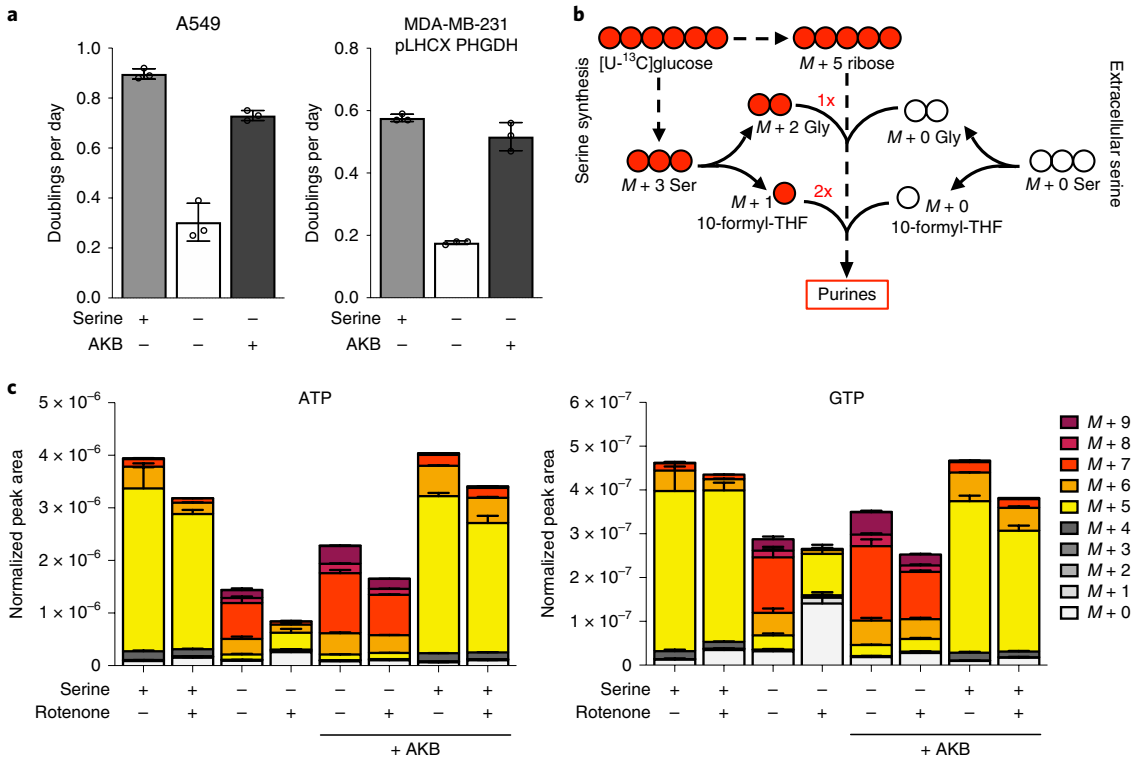

Fig. 4 | Electron acceptors are an endogenous limitation for serine synthesis and proliferation in the absence of exogenous serine. a, Proliferation rates of A549 and PHGDH-expressing MDA-MB-231 cells (pLHCX PHGDH) cultured in serine-replete or serine-free medium with or without AKB as indicated. **b**, Schematic of how [U-^{13}C]glucose carbon can contribute label to serine and purines. Newly synthesized purines incorporate ribose containing 5 ^{13}C-labelled carbons from labelled glucose. If serine that is synthesized from ^{13}C-labelled glucose contributes to purine synthesis, up to 4 additional ^{13}C-labelled carbons can be incorporated, because glycine produced from glucose-derived serine can contribute 2 ^{13}C-labelled carbons, and 10-formyl-THF from glucose-derived serine can contribute up to 2 ^{13}C labels. Thus, $M+5$ labelling suggests that the purine is newly synthesized using exogenous serine, while species with >5 ^{13}C labels suggests that the purine is synthesized using glucose-derived serine. **c**, Total levels and labelling of ATP and GTP from [U-^{13}C]glucose in A549 cells grown with or without serine, 20 nM rotenone and AKB as indicated. Data shown are mean (± s.d.) of three biological replicates.

synthesis, leading to purine depletion over time. Consistent with previous reports, the purine-synthesis intermediates phosphoribosyl-glycinamide (GAR) and 5′-phosphoribosyl-5-aminoimidazole-4-carboxamide (AICAR) also accumulated in serine-deprived cells[10] (Fig. 3d). As these intermediates each precede 1C-requiring reactions in purine synthesis, this accumulation is consistent with insufficient 1C units limiting purine synthesis. Restoring 1C units by supplementing cells with formate alleviated this accumulation (Fig. 3d), as noted previously[10,17].

Salvage of purine nucleobases avoids the demand for serine-derived carbon to synthesize purines de novo. When [5-^{13}C]hypoxanthine was provided, this was the primary carbon contributor to both adenylate and guanylate nucleotides, regardless of serine availability (Fig. 3e and Supplementary Fig. 3b). Importantly, salvage of hypoxanthine rescued purine levels in serine-starved cells. Moreover, providing either formate to restore 1C unit availability or hypoxanthine to directly restore purine levels partially rescued cell proliferation in serine-free medium (Fig. 3f). Formate or hypoxanthine supplementation also improved the proliferation of serine-deprived cells following rotenone or metformin treatment (Fig. 3f, Supplementary Fig. 3c,d and Supplementary Fig. 5b). Importantly, formate or hypoxanthine supplementation did not restore the NAD$^+$/NADH ratio (Supplementary Fig. 4a), suggesting that maintaining purine synthesis is a metabolic requirement downstream of NAD$^+$ availability, and a reason why NAD$^+$ is limiting for cell proliferation.

Serine synthesis requires NAD$^+$ in the cytosol, so coupling this pathway to mitochondrial electron transport requires redox shuttles to transport electrons across the mitochondrial membranes. The malate–aspartate shuttle is one contributor to redox shuttling between the mitochondria and the cytosol. Disrupting this shuttle by knockdown of aspartate–glutamate carrier 1 (AGC1) expression[21] did not affect proliferation of cells grown without exogenous serine, but did increase sensitivity of serine-deprived cells to complex I inhibition (Supplementary Fig. 4b). These data are consistent with the malate–aspartate shuttle being important to maintain cytosolic NAD$^+$ when mitochondrial NAD$^+$ regeneration is impaired.

NAD$^+$ availability can also be affected by nicotinamide salvage. Indeed, inhibiting nicotinamide salvage can inhibit serine synthesis in *PHGDH*-amplified breast cancer cells[16]. We therefore investigated whether nicotinamide salvage can increase oxidized NAD$^+$ availability for serine synthesis. Addition of nicotinamide mononucleotide (NMN) did not restore proliferation of cells cultured without exogenous serine, and did not change the cellular NAD$^+$/NADH ratio (Supplementary Fig. 4c). This may indicate that the NAD$^+$/NADH ratio is a stronger constraint on serine synthesis than is the total amount of NAD(H) in cells.

We next questioned whether basal NAD$^+$ regeneration limits cell proliferation in the absence of exogenous serine. Indeed, increasing NAD$^+$ regeneration by providing AKB increased proliferation of cells cultured in serine-free conditions (Fig. 4a and Supplementary Fig. 5a,b). To evaluate whether NAD$^+$ regeneration constrains purine synthesis in serine-deprived cells, we measured [U-^{13}C]glucose incorporation into purines in cells grown in serine-free or serine-replete medium with or without rotenone. In these experiments, newly synthesized nucleotides are labelled with a mass value of

$M+5$ because the ribose sugar contains 5 ^{13}C carbons from [U-^{13}C] glucose. Moreover, this tracing can distinguish the source of serine used for purine production. When produced from glucose-derived serine, glycine is $M+2$ labelled, and each 1C unit is $M+1$ labelled. Thus, purines with mass values of $M+6$ or greater were produced using glucose-derived serine (Fig. 4b)[11].

By 48 h of labelling, cells cultured in the presence of serine had purines that were mostly $M+5$ labelled (Fig. 4c and Supplementary Fig. 6a–d), suggesting that most of the serine used for purine synthesis in these cells is from the environment. Again, cells grown in the absence of serine had decreased purine pools. Furthermore, because serine-deprived cells must use glucose-derived serine for purine production, their purines had mass values of $M+6$ or greater. Consistent with NAD^+ being limiting for serine synthesis and the production of 1C units for purines, rotenone treatment further decreased purine levels and decreased the levels of purines with mass values of $M+6$ or greater. For both untreated and rotenone-treated cells grown in serine-free medium, addition of AKB increased intracellular purine levels, and increased contribution of glucose-derived serine to purines, resulting in increased labelling of purines with mass values of $M+6$ or greater. Notably, expression of serine synthesis enzymes was necessary for this rescue, as MDA-MB-231 cells required PHGDH expression to produce purines using synthesized serine (Supplementary Fig. 6b). These data confirm that increasing NAD^+ availability can restore purine production using serine synthesized from glucose, and suggest that demand for NAD^+ constrains the use of serine synthesis to support purine production and allow maximal cell proliferation.

The metabolic network available to cancer cells is defined by the enzymes and regulatory factors expressed and thus is influenced both by the cell type that gave rise to the cancer, and by the genetic and signalling changes that drive the cancer[22,23]. In addition, cancer cells in different tissues are exposed to different nutrient environments[24]. This suggests that different cancers experience different metabolic constraints, and might underlie why cancers show differential sensitivity to drugs targeting metabolic processes predicted to be important in all proliferating cells[14,25].

We find that the extent to which cells can utilize the serine synthesis pathway is dictated by NAD^+ availability. Mitochondrial respiration allows net regeneration of NAD^+ from NADH, and this ability to regenerate NAD^+ is an important way that respiration supports cell proliferation[12–14]. Previous work has focused on aspartate production as a precursor for proteins and nucleotides that could be limited by NAD^+ regeneration[12,13,26]. The finding that serine metabolism for purine synthesis can also be limited by NAD^+ regeneration demonstrates that aspartate production is not the only important way that NAD^+ supports proliferation. Many NAD^+-consuming reactions compete for NAD^+, and whether production of aspartate, the generation of serine-derived 1C units, or other processes requiring NAD^+ as a cofactor are more limiting will depend on the cancer context. For example, if environmental serine is limited, then NAD^+ consumption in serine synthesis might become required and select for adaptations to circumvent other NAD^+-utilizing pathways.

The demand for extracellular serine is consistent with studies showing that dietary serine limitation can slow the growth of some, but not all, tumours. Indeed, dietary serine limitation appears to be more effective for slowing the growth of tumours arising in tissues with lower serine content[6,9]. Low-serine tissue environments appear to select for tumours that genetically upregulate serine synthesis[6]. While this increases intracellular serine and supports faster tumour growth[6], the requirement for serine synthesis in these tumours could render them vulnerable to NAD^+ depletion. Further, high rates of serine synthesis in these tumours might make NAD^+ less available for other pathways needed to synthesize oxidized biomass, resulting in other metabolic limitations. Similarly, our data suggest that tumours growing in environments where NAD^+ availability is more limited may be more susceptible to serine deprivation. In line with this idea, a serine-deficient diet enhances the efficacy of metformin treatment in a mouse allograft cancer model[15]. Recognizing that forcing increased serine production can synergize with drugs, such as metformin, that inhibit NAD^+ regeneration, not because they limit the carbon available for ATP production[15] but rather because they cause a redox imbalance, suggests that other NAD^+-depleting drugs could also enhance response to dietary serine limitation. By extension, a better understanding of how differential pathway use by cancer cells creates metabolic liabilities could suggest additional opportunities to target metabolism for therapeutic benefit.

Methods

Cell culture. All cell lines were cultured in Dulbecco's modified Eagle's medium (DMEM) (GIBCO) supplemented with 10% heat inactivated foetal bovine serum at 37 °C with 5% CO_2. Pyruvate or nucleotides were not included in the culture medium, except when indicated. Concentrations of metabolites added to treatment medium are listed in Supplementary Table 1.

Proliferation rates. Cells were trypsinized, counted and plated in 6-well plates (Denville) in 2 ml DMEM with 10% FBS and incubated overnight. Cells were plated at 20,000 cells per well (A549, 143B, H1299) or 40,000 (MDA-MB-468, MDA-MB-231, T.T, Carney, BT-20, H522, HS578T) cells per well in 6-well plates. The following day, one 6-well plate for each cell line was counted to determine the initial number of cells at the time of treatment. Cells were washed three times with 2 ml PBS and 4 ml of treatment medium was added. Treatment medium was made with 10% dialyzed FBS. Serine-free medium was made by adding a mix of amino acids at DMEM concentrations lacking serine to DMEM without pyruvate or amino acids. The number of cells seeded for each cell line allowed for exponential growth over the course of the assay. After 4 days of treatment, final cell counts were measured using a Cellometer. The following formula was used to calculate proliferation rate:

Doublings per day = $\log_2$ (final cell count/initial cell count)/4, where the final cell count was on day 5, and the initial cell count was on day 1.

Western blots. 10^6 cells were plated in 10-cm plates and incubated overnight to allow cells to adhere. The following day, cells were washed three times with PBS, and 10 ml of treatment medium containing 10% dialyzed FBS was added. After culturing cells for 24 h in treatment medium, protein lysates were prepared: cells were trypsinized, pelleted and washed twice with PBS. Cells were then resuspended in ice-cold RIPA buffer with protease inhibitor. Lysed cells were centrifuged at maximum speed at 4 °C, and the protein lysate supernatant was removed and stored at −80 °C. Proteins were separated using SDS–polyacrylamide gel electrophoresis (SDS–PAGE) (12% acrylamide gels) and transferred to a nitrocellulose membrane using a wet transfer method. Membranes were blocked for 60 min using 5% bovine serum albumin (BSA) in Tris buffered saline with Tween (TBST). Membranes were incubated in primary antibody overnight at 4 °C. The following primary antibodies were used: vinculin (Cell Signaling Technology), PHGDH (Sigma), PSAT (Abnova), and PSPH (Sigma Prestige). Antibodies were diluted in 5% BSA in TBST (vinculin and PSAT, 1:1,000; PHGDH and PSPH, 1:500). The following day, membranes were washed three times with TBST on a rocker for 10 min. Secondary antibodies were applied for 60 min. Anti-rabbit (Cell Signaling Technology) secondary antibody was used at a dilution of 1:5,000 and anti-mouse (Cell Signaling Technology) secondary antibody was used at a dilution of 1:10,000. Membranes were then washed again three times with TBST for 10 min on a rocker. Signal was detected using film. Uncropped Western blots are shown in Supplementary Figure 7.

Liquid chromatography–mass spectrometry analysis. 100,000 cells were plated in 6-well plates in 2 ml DMEM with 10% FBS and were incubated overnight. The following day, cells were washed three times with PBS, and 4 ml of treatment medium was added. All treatment media were made with 10% dialyzed FBS. After the indicated time period, polar metabolites were extracted from cells: plates were placed on ice, cells were washed with ice-cold blood bank saline, and 500 µl of ice-cold 80% methanol in water with 250 nM $^{13}C/^{15}N$-labelled amino acid standards (Cambridge Isotope Laboratories, Inc.) was added to each well. Cells were scraped, and each sample was vortexed for 10 min at 4 °C, and then centrifuged at maximum speed for 10 min at 4 °C. Samples were dried under nitrogen gas and resuspended in 25 µl of a 50/50 acetonitrile/water mixture. Metabolites were measured using a Dionex UltiMate 3000 ultra-high performance liquid chromatography system connected to a Q Exactive benchtop Orbitrap mass spectrometer, equipped with an Ion Max source and a HESI II probe (Thermo Fisher Scientific). Samples were separated by chromatography by injecting 2–10 µl of sample on a SeQuant ZIC-pHILIC Polymeric column (2.1 × 150 mm 5 µM, EMD Millipore). Flow rate was set to 150 µl min^{-1}, temperatures were set to 25 °C for column compartment and 4 °C for autosampler sample tray. Mobile Phase A consisted of 20 mM ammonium carbonate, 0.1% ammonium hydroxide. Mobile Phase B was

100% acetonitrile. The mobile phase gradient (%B) was set in the following protocol: 0–20 min.: linear gradient from 80% to 20% B; 20–20.5 min.: linear gradient from 20% to 80% B; 20.5–28 min.: hold at 80% B. Mobile phase was introduced into the ionization source set to the following parameters: sheath gas = 40, auxiliary gas = 15, sweep gas = 1, spray voltage = −3.1 kV, capillary temperature = 275 °C, S- lens RF level = 40, probe temperature = 350 °C. Metabolites were monitored in full-scan, polarity-switching, mode. An additional narrow range full-scan (220–700 *m/z*) in negative mode only was included to enhance nucleotide detection. The resolution was set at 70,000, the AGC target at 1,000,000 and the maximum injection time at 20 msec. Relative quantitation of metabolites was performed with XCalibur QuanBrowser 2.2 (Thermo Fisher Scientific) using a 5 ppm mass tolerance and referencing an in-house retention time library of chemical standards. Metabolite measurements were normalized to the internal $^{13}C/^{15}N$-labelled amino acid standard and to cell number.

Metabolomic data analysis. 100,000 cells were plated in 6-well dishes and allowed to adhere overnight. The following day, cells were washed three times with PBS and 4 ml of the specified medium was added. After 48 h, polar metabolites were extracted and analysed using a Dionex UltiMate 3000 ultra-high performance liquid chromatography system connected to a Q Exactive benchtop Orbitrap mass spectrometer, as described in 'Liquid chromatography–mass spectrometry analysis'. Metabolite peak integration was performed as above using XCalibur QuanBrowser 2.2, and peak areas were normalized to an internal standard ($^{13}C/^{15}N$-labelled amino acid standard) and to cell number. Differential and statistical analysis was performed using MetaboAnalystR. The following parameters were used: data normalization: normalization to sample median; data transformation: log normalization; data scaling: autoscaling. Hierarchical clustering in MetaboAnalystR was performed using the following parameters: similarity measure: Euclidean distance; clustering algorithm: Ward's linkage.

NAD$^+$/NADH measurements. NAD$^+$/NADH measurements were performed using the NAD/NADH Glo Assay (Promega) with a modified version of manufacturer instructions, as reported previously[13]. Cells were plated as was done for proliferation assays and incubated overnight. Cells were treated as indicated for 6 h prior to preparation of cell extracts. For extraction, cells were washed 3 times in ice cold PBS, and extracted in 100 µl ice-cold lysis buffer (1% dodecyltrimethylammonium bromide (DTAB) in 0.2 N NaOH diluted 1:1 with PBS). Each sample was flash-frozen in liquid nitrogen and immediately stored at −80 °C. To measure NADH, 20 µl of sample was moved to PCR tubes and incubated at 75 °C for 30 min, where basic conditions selectively degrade NAD$^+$. To measure NAD$^+$, 20 µl of the samples was moved to PCR tubes containing 20 µl lysis buffer and 20 µl 0.4 N HCl and incubated at 60 °C for 15 min, where acidic conditions selectively degrade NADH. Samples were then allowed to equilibrate to room temperature and quenched by neutralizing with 20 µl 0.25 M Tris in 0.2 N HCl (for NADH) or 20 µl 0.5 M Tris base (for NAD$^+$). Manufacturer instructions were followed thereafter to measure NAD$^+$/NADH.

Reporting Summary. Further information on research design is available in the Nature Research Reporting Summary linked to this article.

Data availability

The raw data that support the findings of this study are available from the corresponding author upon request. Raw data for Fig. 1a, Supplementary Figure 1c and Supplementary Figure 2a (uncropped western blots) are shown in Supplementary Figure 7.

Received: 19 December 2018; Accepted: 7 August 2019;
Published online: 16 September 2019

References

1. Hosios, A. M. et al. Amino acids rather than glucose account for the majority of cell mass in proliferating mammalian cells. *Dev. Cell* **36**, 540–549 (2016).
2. Yang, M. & Vousden, K. H. Serine and one-carbon metabolism in cancer. *Nat. Rev. Cancer* **16**, 650–662 (2016).
3. Ducker, G. S. & Rabinowitz, J. D. One-carbon metabolism in health and disease. *Cell Metab.* **25**, 27–42 (2017).
4. Newman, A. C. & Maddocks, O. D. K. One-carbon metabolism in cancer. *Br. J. Cancer* **116**, 1499–1504 (2017).
5. Possemato, R. et al. Functional genomics reveal that the serine synthesis pathway is essential in breast cancer. *Nature* **476**, 346–350 (2011).
6. Sullivan, M. R. et al. Increased serine synthesis provides an advantage for tumors arising in tissues where serine levels are limiting. *Cell Metab.* **29**, P1410–1421 (2019).
7. Mattaini, K. R., Sullivan, M. R. & Heiden, M. G. V. The importance of serine metabolism in cancer. *J. Cell Biol.* **214**, 249–257 (2016).
8. DeNicola, G. M. et al. NRF2 regulates serine biosynthesis in non-small cell lung cancer. *Nat. Genet.* **47**, 1475–1481 (2015).
9. Maddocks, O. D. K. et al. Modulating the therapeutic response of tumours to dietary serine and glycine starvation. *Nature* **544**, 372–376 (2017).
10. Labuschagne, C. F., van den Broek, N. J. F., Mackay, G. M., Vousden, K. H. & Maddocks, O. D. K. Serine, but not glycine, supports one-carbon metabolism and proliferation of cancer cells. *Cell Rep.* **7**, 1248–1258 (2014).
11. Pacold, M. E. et al. A PHGDH inhibitor reveals coordination of serine synthesis and 1-carbon unit fate. *Nat. Chem. Biol.* **12**, 452–458 (2016).
12. Birsoy, K. et al. An essential role of the mitochondrial electron transport chain in cell proliferation is to enable aspartate synthesis. *Cell* **162**, 540–551 (2015).
13. Sullivan, L. B. et al. Supporting aspartate biosynthesis is an essential function of respiration in proliferating cells. *Cell* **162**, 552–563 (2015).
14. Gui, D. Y. et al. environment dictates dependence on mitochondrial complex I for NAD$^+$ and aspartate production and determines cancer cell sensitivity to metformin. *Cell Metab.* **24**, 716–727 (2016).
15. Gravel, S.-P. et al. Serine deprivation enhances antineoplastic activity of biguanides. *Cancer Res.* **74**, 7521–7533 (2014).
16. Murphy, J. P. et al. The NAD+ Salvage Pathway Supports PHGDH-driven serine biosynthesis. *Cell Rep.* **24**, 2381–2391.e5 (2018).
17. Bao, X. R. et al. Mitochondrial dysfunction remodels one-carbon metabolism in human cells. *eLife* **5**, (2016).
18. Hosios, A. M. & Heiden, M. G. V. The redox requirements of proliferating mammalian cells. *J. Biol. Chem.* **293**, 7490–7498 (2018).
19. Lewis, C. A. et al. Tracing compartmentalized NADPH metabolism in the cytosol and mitochondria of mammalian cells. *Mol. Cell* **55**, 253–263 (2014).
20. Ducker, G. S. et al. Reversal of cytosolic one-carbon flux compensates for loss of the mitochondrial folate pathway. *Cell Metab.* **23**, 1140–1153 (2016).
21. Alkan, H. F. et al. Cytosolic Aspartate Availability Determines Cell Survival When Glutamine Is Limiting. *Cell Metab.* **28**, 706–720.e6 (2018).
22. Mayers, J. R. et al. Tissue of origin dictates branched-chain amino acid metabolism in mutant Kras-driven cancers. *Science* **353**, 1161–1165 (2016).
23. Vander Heiden, M. G. & DeBerardinis, R. J. Understanding the intersections between metabolism and cancer biology. *Cell* **168**, 657–669 (2017).
24. Davidson, S. M. et al. Environment impacts the metabolic dependencies of ras-driven non-small cell lung cancer. *Cell Metab.* **23**, 517–528 (2016).
25. Muir, A. et al. Environmental cystine drives glutamine anaplerosis and sensitizes cancer cells to glutaminase inhibition. *eLife* **6**, e27713 (2017).
26. Sullivan, L. B. et al. Aspartate is an endogenous metabolic limitation for tumour growth. *Nat. Cell Biol.* **20**, 782–788 (2018).

Acknowledgements

We thank members of the Vander Heiden Lab for helpful discussions. We thank H. Furkan Alkan for providing the A549 shAGC1 cells. F.F.D. acknowledges support from the NIH (F31CA236036). M.G.V.H. acknowledges support from a Faculty Scholar grant from the Howard Hughes Medical Institute, SU2C, a division of the Entertainment Industry Foundation, the Lustgarten Foundation, the MIT Center for Precision Cancer Medicine, the Ludwig Center at MIT and the NIH (R01CA201276, R01CA168653 and P30CA14051).

Author contributions

F.F.D. performed most experiments. F.F.D. and C.A.L. performed metabolite tracing experiments and LCMS data analysis. B.P.F. and C.A.L. performed the [6-^{13}C]glucose and [3-^{13}C]serine tracing experiment. F.F.D. and M.G.V.H. designed the study and wrote the manuscript.

Competing interests

The authors are aware of no direct conflicts with the topic of the paper; however M.G.V.H. discloses that he is a scientific advisor and/or shareholder of Agios Pharmaceuticals, Aeglea Biotherapeutics and Auron Therapeutics. B.P.F. discloses he is a founder of Mythic Therapeutics.

Additional information

Supplementary information is available for this paper at https://doi.org/10.1038/s42255-019-0108-x.

Reprints and permissions information is available at www.nature.com/reprints.

Correspondence and requests for materials should be addressed to M.G.V.

Peer review information Primary Handling Editor: Ana Mateus.

Publisher's note Springer Nature remains neutral with regard to jurisdictional claims in published maps and institutional affiliations.

nature research

Corresponding author(s): Matthew Vander Heiden

Last updated by author(s): Aug 5, 2019

Reporting Summary

Nature Research wishes to improve the reproducibility of the work that we publish. This form provides structure for consistency and transparency in reporting. For further information on Nature Research policies, see Authors & Referees and the Editorial Policy Checklist.

Statistics

For all statistical analyses, confirm that the following items are present in the figure legend, table legend, main text, or Methods section.

n/a	Confirmed	
☐	☒	The exact sample size (*n*) for each experimental group/condition, given as a discrete number and unit of measurement
☐	☒	A statement on whether measurements were taken from distinct samples or whether the same sample was measured repeatedly
☒	☐	The statistical test(s) used AND whether they are one- or two-sided *Only common tests should be described solely by name; describe more complex techniques in the Methods section.*
☒	☐	A description of all covariates tested
☐	☒	A description of any assumptions or corrections, such as tests of normality and adjustment for multiple comparisons
☐	☒	A full description of the statistical parameters including central tendency (e.g. means) or other basic estimates (e.g. regression coefficient) AND variation (e.g. standard deviation) or associated estimates of uncertainty (e.g. confidence intervals)
☒	☐	For null hypothesis testing, the test statistic (e.g. *F*, *t*, *r*) with confidence intervals, effect sizes, degrees of freedom and *P* value noted *Give P values as exact values whenever suitable.*
☒	☐	For Bayesian analysis, information on the choice of priors and Markov chain Monte Carlo settings
☐	☒	For hierarchical and complex designs, identification of the appropriate level for tests and full reporting of outcomes
☒	☐	Estimates of effect sizes (e.g. Cohen's *d*, Pearson's *r*), indicating how they were calculated

Our web collection on statistics for biologists contains articles on many of the points above.

Software and code

Policy information about availability of computer code

Data collection	No software was used to collect data.
Data analysis	Mass spectrometry data was analyzed with XCalibur QuanBrowser 2.2. Hierarchical clustering of metabolomics data was performed with MetaboAnalystR.

For manuscripts utilizing custom algorithms or software that are central to the research but not yet described in published literature, software must be made available to editors/reviewers. We strongly encourage code deposition in a community repository (e.g. GitHub). See the Nature Research guidelines for submitting code & software for further information.

Data

Policy information about availability of data

All manuscripts must include a data availability statement. This statement should provide the following information, where applicable:

- Accession codes, unique identifiers, or web links for publicly available datasets
- A list of figures that have associated raw data
- A description of any restrictions on data availability

Ucropped Western blots are shown in Supplementary Figure 7. All other data generated that support the findings of this study are available from the corresponding author upon request.

Field-specific reporting

Please select the one below that is the best fit for your research. If you are not sure, read the appropriate sections before making your selection.

☒ Life sciences ☐ Behavioural & social sciences ☐ Ecological, evolutionary & environmental sciences

For a reference copy of the document with all sections, see nature.com/documents/nr-reporting-summary-flat.pdf

Life sciences study design

All studies must disclose on these points even when the disclosure is negative.

Sample size	Experiments were performed using sample sizes based on standard protocols in the field. No statistical test was performed to predetermine sample size.
Data exclusions	No data was excluded.
Replication	All experiments were repeated multiple times, and results were reproducible. Experimental results shown in bar graphs are from 3 biological replicates. For experiments where representative data is shown (i.e. Western blots), the experiment was repeated multiple times with consistent results.
Randomization	This is not relevant to the study, as all experiments were done using human cell lines. No experiments involved allocation of different samples, organisms, or participants into experimental groups.
Blinding	Blinding was not relevant to the study because no experiments involved allocation of different samples, organisms, or participants into experimental groups.

Reporting for specific materials, systems and methods

We require information from authors about some types of materials, experimental systems and methods used in many studies. Here, indicate whether each material, system or method listed is relevant to your study. If you are not sure if a list item applies to your research, read the appropriate section before selecting a response.

Materials & experimental systems

n/a	Involved in the study
☐	☒ Antibodies
☐	☒ Eukaryotic cell lines
☒	☐ Palaeontology
☒	☐ Animals and other organisms
☒	☐ Human research participants
☒	☐ Clinical data

Methods

n/a	Involved in the study
☒	☐ ChIP-seq
☒	☐ Flow cytometry
☒	☐ MRI-based neuroimaging

Antibodies

Antibodies used	Primary antibodies: Vinculin (Cell Signaling Technology, 13901, 1:1000, Lot 5), PHGDH (Sigma Prestige, HPA024031, 1:500 Lot QC24006), PSAT (Abnova, H00029968-A01, 1:1000, Lot 09294), and PSPH (Sigma Prestige, HPA020376, 1:500, Lot A39815). Secondary antibodies: HRP-linked anti-rabbit IgG (Cell Signaling Technology, 7074, 1:5000, Lot 27), HRP-linked anti-mouse IgG (Cell Signaling Technology, 7076, 1:10000, Lot 32).
Validation	Antibodies were validated by the suppliers. Validation and antibody profiles are supplied in the links below. Vinculin: https://www.cellsignal.com/products/primary-antibodies/vinculin-e1e9v-xp-rabbit-mab/13901 PHGDH: https://www.sigmaaldrich.com/catalog/product/sigma/hpa024031?lang=en&region=US The PHGDH antibody was also validated using a cell line that naturally does not strongly express PHGDH: a strong band was present only when PHGDH was exogenously expressed in this cell line. PSAT: http://www.abnova.com/products/products_detail.asp?catalog_id=H00029968-A01 PSPH: https://www.sigmaaldrich.com/catalog/product/sigma/hpa020376?lang=en&region=US HHRP-linked anti-rabbit IgG:

https://www.cellsignal.com/products/secondary-antibodies/anti-rabbit-igg-hrp-linked-antibody/7074

HRP-linked anti-mouse IgG:
https://www.cellsignal.com/products/secondary-antibodies/anti-mouse-igg-hrp-linked-antibody/7076

Eukaryotic cell lines

Policy information about cell lines

Cell line source(s)	All cell lines (A549, 143B, H1299, MDA-MB-468, MDA-MB-231, T.T, Carney, BT-20, H522, and HS578T) were obtained from ATCC.
Authentication	The identities of all cells were authenticated by satellite tandem repeat testing and referenced to ATCC values.
Mycoplasma contamination	All cell lines tested negatively for mycoplasma.
Commonly misidentified lines (See ICLAC register)	None of our cell lines are listed in ICLAC as commonly misidentified cell lines.